Quantum Poincaré sections for two-dimensional billiards

Bruno Crespi,* Gabriel Perez,† and Shau-Jin Chang
Department of Physics, University of Illinois at Urbana-Champaign, 1110 West Green Street, Urbana, Illinois 61801
(Received 27 January 1992; revised manuscript received 2 July 1992)

We show a method to extract the quantum Poincaré section corresponding to an eigenstate of a two-dimensional billiard. This quantum Poincaré section is given in terms of the Birkhoff variables of the problem.

PACS number(s): 05.45.+b, 03.65.Ge

I. INTRODUCTION

In recent times the dynamics of two-dimensional (2D) billiards has attracted great attention [1]. These are systems made of a free point particle moving in a bounded 2D region Ω. The motion of billiards shows a rich variety of phenomena, depending on the shape of their walls. Their dynamical behavior ranges from chaotic to integrable. A completely chaotic behavior appears in the stadium billiard [2], and in the Sinai billiard [3]. This makes billiards one of the simplest nondriven Hamiltonian systems that can show chaos. There is an intermediate regime of nonintegrable billiards where regular orbits (KAM tori) and chaotic trajectories coexist. In particular, Lazutkin and others [4] have proven that any convex billiard whose boundary is $\mathbb{C}^n$, $n \geq 6$, contains an infinite family of regular orbits, and that this family has nonzero measure in phase space. These regular orbits run close to the boundary and accumulate upon it, and are called the *whispering gallery* of the billiard. Regular orbits also exist in billiards whose boundaries have discontinuous curvature [5], where the KAM theorem no longer applies. There is also a family of completely integrable billiards, namely the billiards with elliptic boundaries. Here both the energy and the product of the angular momenta around the two foci are conserved.

The corresponding quantum problem in configuration space is straightforward, and reduces to the solution of the Helmholtz equation

$$\nabla^2\psi + k^2\psi = 0, \tag{1}$$

with boundary conditions $\psi|_{\partial\Omega} = 0$. The relevant eigennumber is the dimensionless combination $\sqrt{A}k$, where A is the area of Ω. This quantization problem has been studied recently by many authors [6–9], and has become one of the paradigms of "quantum chaology." There has been a large amount of work on the quantum wave functions which show the influence of the classical unstable periodic orbits (scars [7]), and on the energy spectrum [8] which evolves from Poissonian to Gaussian as the nonintegrability parameter of the system increases.

In this report we want to show how to cast the information contained in the quantum wave function into a (2D) phase-space representation (Poincaré section), in terms of the Birkhoff variables of the system. This gives us a new way of establishing the connection between different wave functions and their underlying classical trajectories, in the large action limit.

II. REVIEW OF BIRKHOFF VARIABLES

For the classical billiard all dynamical information is contained in the canonical Birkhoff variables [10]. These are defined for every bounce of the particle in the walls by the following two parameters: the normalized oriented arc length s measured from some reference point on the wall to the site of the bounce ($0 \leq s < 1$), and the cosine c of the angle between the outgoing direction of the particle and the oriented tangent to the wall on the point of impact ($-1 \leq c \leq 1$). The dynamics of the billiard establishes a mapping between these variables

$$s_n, c_n \rightarrow s_{n+1}, c_{n+1}, \tag{2}$$

which for convex $\mathbb{C}^1$ boundaries is continuous and area preserving. These two variables correspond to position and its associated momentum (p_s), measured over the boundary, in some curved coordinate system where the boundary itself has a constant coordinate value. We will take this coordinate system to be orthogonal and continuously deformable into a polar system. To show in a simple and intuitive way how to define these coordinates we can use 2D electrostatics. We just set the wall of the billiard to be a grounded conductor and put a point charge anywhere in its interior. This generates an orthogonal system given by the equipotentials and the field lines. The coordinate along the equipotential is periodic, analogous to the angle in the polar system. We measure it from 0 to 1 and in such a way that it coincides with the normalized arc length s on the wall of the billiard. The coordinate along the field lines is analogous to r in the polar system and will be called ρ, with the convention $\rho = 1$ at the boundary. The variable c is defined by $c \equiv p_s/p$, where p is the magnitude of the conserved total momentum and p_s is its component along s. Notice that there is no periodicity in p_s, and obviously none in c.

The mapping of the Birkhoff variables in this coordinate system is a Poincaré mapping, where we fix $\rho = 1$. The magnitude of p_ρ is defined by energy conservation, and its sign changes from + to − upon impact. The phase

space generated by the pair (s,p_s) is the cylinder $S_1 \times R$, but conservation of energy means that for any given total momentum p only the section $-p \leq p_s \leq p$ is allowed for the Poincaré section. Time-reversal symmetry ensures that there is an invariance in the mapping under the reversal $p_s \to -p_s$, making the Poincaré section symmetric with respect to the line $c = 0$.

III. QUANTUM POINCARÉ SECTIONS AND HUSIMI DISTRIBUTIONS

Since the Helmholtz equation is in general not separable in the ρ, s variables, there is no known way of quantizing the billiard directly in terms of the Birkhoff variables. Here we show a method to get the quantum Poincaré section (QPS) corresponding to any given eigenstate of a billiard, once it has been quantized in configuration space. Let us start with a simple example. Take a circular billiard of radius 1. For this case there is an immediate separation of the wave functions in angular and radial parts. The real eigenfunctions (ignoring normalization) are

$$\psi(r,\theta) = J_m(k_{mn}r)\cos(m\theta + \phi). \tag{3}$$

Here $\rho = r$, $s = \theta/(2\pi)$, and ϕ is an arbitrary phase. To build a quantum equivalent of the Poincaré section we need to know the probability of finding the particle close to the border, at an angle θ and with angular momentum p_θ. The fact that we can separate variables makes this task easy, since the probability for any given value of r depends only on θ. Therefore, the angular part of the wave function alone can be used to construct a distribution in the pair $(s,\ p_s)$. To obtain this reduced phase space information we use Husimi distributions [11], in preference to Wigner functions [12], which are not strictly positive and that for compact variables are different from zero only on δ stripes.

The Husimi distribution for a real one-dimensional space is given by

$$H_\psi(q_0,k_0) = |\langle q_0,k_0 \mid \psi\rangle|^2, \tag{4}$$

where $\mid q_0,k_0\rangle$ is a coherent state centered around q_0 in configuration space and around $k_0 \equiv p_0/\hbar$ in wave-number space. The position representation is

$$\langle q \mid q_0,k_0\rangle = \left(\frac{1}{\pi\sigma^2}\right)^{1/4} \exp\left[-\frac{(q-q_0)^2}{2\sigma^2} + ik_0(q-q_0)\right], \tag{5}$$

where $\sigma/\sqrt{2}$ is the dispersion in position, and $1/(\sigma\sqrt{2})$ is the dispersion in wave number. For a space topologically equivalent to a circle and in terms of a periodic variable such as the angle θ in the circular billiard, we can introduce a periodic coherent state as [13]

$$\langle q \mid q_0,k_0\rangle_{\rm per} = \sum_{n=-\infty}^{\infty} \langle q-n \mid q_0,k_0\rangle, \tag{6}$$

with $0 \leq q,q_0 < 1$. It is important to note that the coherent state so constructed is periodic only in the q_0 variable, but not in the k_0 variable. The space defined by (q_0,k_0) is a cylinder and is not bounded in the k_0 direction. Generalized coherent states for a more general compact space have been studied extensively in Refs. [14, 15].

Using these coherent states we can obtain a Husimi distribution for the angular part of the eigenfunctions of the circular billiard. We get (ignoring normalization and choosing $\phi = 0$)

$$\begin{aligned} H(\theta,k_\theta) &= |\langle \theta,k_\theta \mid \cos m\theta\rangle_{\rm per}|^2 \\ &= e^{-(k_\theta-m)^2\sigma^2} + e^{-(k_\theta+m)^2\sigma^2} \\ &\quad +2\,e^{-(m^2+k_\theta^2)\sigma^2}\cos(2m\theta). \end{aligned} \tag{7}$$

This function is strongly peaked around the lines $k_\theta = \pm m$, with a very weak oscillatory dependence on θ. For an eigenstate with total momentum $p = \hbar k_{mn}$ the Poincaré section in s and c peaks around $c = m/k_{mn} < 1$, since the smallest root of the Bessel function $J_m(\rho)$ is always larger than m. For large m this smallest root [16], $k_{m1} \approx m + (1.86\ldots)m^{1/3} + \mathcal{O}(1)$, approaches m. This means that the whispering gallery, which has $c \approx \pm 1$, appears in the circular billiard only for some highly exited states. This behavior can be found also in billiards with other shapes.

We cannot perform this simple separation of the wave function for billiards with arbitrary shapes. There is, however, an approximated separation of the wave function near the boundary, because the boundary is a nodal line. Around $\rho = 1$ we can write

$$\psi(\rho,s)|_{\rho\approx 1} = 0 + \left.\frac{\partial\psi(\rho,s)}{\partial\rho}\right|_{\rho=1}(\rho-1) + \mathcal{O}((\rho-1)^2) + \cdots, \tag{8}$$

which means that locally $\psi(\rho,s)$ can be separated to first order. Therefore at the boundary we can define

$$S(s) \equiv \left.\frac{\partial\psi(\rho,s)}{\partial\rho}\right|_{\rho=1} = \nabla\psi\cdot\hat{\rho}|_{\rho=1}. \tag{9}$$

This quantity gives us the information we need to construct the Husimi distribution for the Birkhoff variables. We just compute

$$H_S(s,k_s) = \left|\int_0^1 ds'\langle s,k_s \mid s'\rangle_{\rm per} S(s')\right|^2, \tag{10}$$

and then normalize k_s by the wave-number eigenvalue k to obtain c. Notice that the simpler approach given by $S(s) = \psi(\rho,s)|_{\rho=1}$ is meaningless because this quantity vanishes identically on the boundary.

We need to make some comments on the relation between our quantum eigenfunctions and the classical Birkhoff surface section map. We have solved the time-independent quantum eigenfunctions which lead to invariant Husimi distributions on the surface section. The classical counterpart of this invariant Husimi distribution is an invariant solution to the Liouville equation of the corresponding billiard system. Our Husimi distributions are automatically invariant under the QPS mapping. On

the other hand, we have not succeeded in constructing an explicit quantum evolution operator which maps a time-dependent Husimi distribution forward with the classical surface of the section map. This quantum evolution operator is not an equal-time map and we find no simple way of constructing it. We can in principle study the action of this quantum evolution operator on a localized state by constructing a wave packet on the surface section out of our eigenfunctions and follow its evolution. However, since we are using a finite $\hbar$, the wave functions tend to spread very fast, which makes the numerical study impractical.

IV. NUMERICAL RESULTS

The previously described method to find the QPS for billiards has been tried in a particular deformation of the circle. This billiard is given by the closed branch of the solutions of the equation

$$x^2 + y^2 + \epsilon x^3 = 1. \tag{11}$$

For $\epsilon = 0.2$ the classical phase space is shown in Fig. 1. This phase space shows the coexistence of a large chaotic orbit and some regular orbits. There is a period-2 window centered at $c = 0$, which appears as a stable vertical trajectory in configuration space. We can also see clearly a stable period-3 window and the stable whispering gallery of orbits close to the boundary, forming a band near $c = \pm 1$. There are also some higher order stable windows with smaller measure in phase space. If we increase ϵ the measure of the chaotic orbit increases, but the stable period-2 window around $c = 0$ does not disappear completely. At the value $\epsilon = \sqrt{4/27}$ the two branches of the solution of Eq. (11) touch at the point $x = -\sqrt{3}$, $y = 0$, which gives a discontinuity in the curvature of the border. Beyond this value of ϵ Eq. (11) does not have closed-curve solutions.

To solve the quantum problem in configuration space

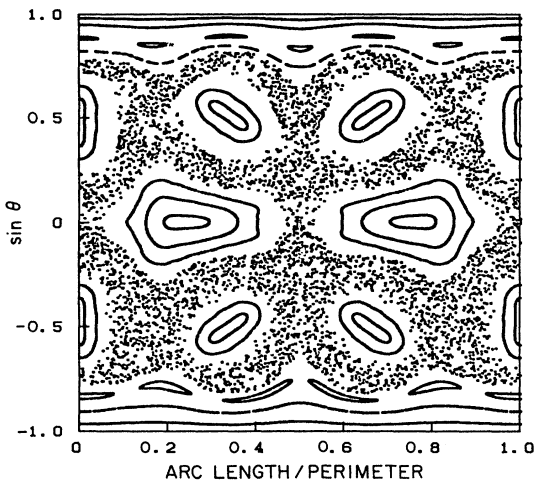

FIG. 1. Classical Poincaré section for the deformed circular billiard $x^2 + y^2 + \epsilon x^3 = 1$, $\epsilon = 0.2$.

we apply a simple implementation of the diagonalization algorithm currently used [8]. We show a few examples of the results in Figs. 2 and 3. Figure 2 shows 10 eigenstates of the billiard, with $30.0 \leq \sqrt{A}k \leq 31.3$. These are all the even eigenstates in this k region, and are listed according to increasing energy. For completeness, we include these eigenvalues in Table I. Figures 2(a) and 2(e) show the scars due to vertical stable period-2 windows, and Figs. 2(b) and 2(g) those of stable period-3 windows. The largest probability densities are found in all these cases around the caustics of the classical trajectories. The caustics corresponding to windows in 2(a) and 2(b) have swallowtail foldings, a feature that affects the associated wave functions only for large values of k. Figure 2(c) shows eigenfunctions associated with the whispering gallery. Figure 2(d) follows an unstable three cycle and Fig. 2(j) shows a scar of the unstable horizontal period-2 cycle. Finally, Figs. 2(f), 2(h), and 2(i) show seemingly chaotic eigenfunctions. All different types of classical motion are reflected in the structure of the wave functions contained in a small range of wave numbers. For larger k we obtain the same types of wave functions, with higher resolution (sharper caustics, clearly defined swallow tails), and some other wave functions associated with stable windows of higher periods.

The QPS's of the wave functions shown before are given in Fig. 3. Here we have chosen σ so as to have symmetric dispersion ($\Delta k/2k_0 = \Delta s/s$). There is a very good correlation between the different QPS's and the quantum-classical correspondence we have found between wave functions and trajectories. In particular, the QPS's of those orbits identified with classical periodic windows fall in the sections of phase space corresponding to the associated stable islands. As shown by the figures, the peaks of the QPS shown in Figs. 3(a) and 3(e) fall roughly in the periphery and the center of the period-2 island, and in Figs. 3(b) and 3(g) in the periphery and the center of the period-3 island, respectively. Those of the wave functions shown in Fig. 3(c) fall on the whispering gallery bands. More interesting are the cases of the irregular eigenfunctions. The QPS shown in Fig. 3(d) follows closely the unstable 3-cycle. The QPS for the unstable period-2, given in Fig. 3(j), peaks strongly on the hyperbolic 2-cycle, giving a scar which is much better de-

TABLE I. Even eigenvalues for the deformed billiard in the range $30 \leq \sqrt{A}k \leq 31.3$. The label denotes the corresponding figure in Figs. 2 and 3

Label	$\sqrt{A}k$
(a)	30.1968
(b)	30.2377
(c)	30.3726
(d)	30.4154
(e)	30.5660
(f)	30.5980
(g)	30.7634
(h)	30.9611
(i)	31.0305
(j)	31.2989

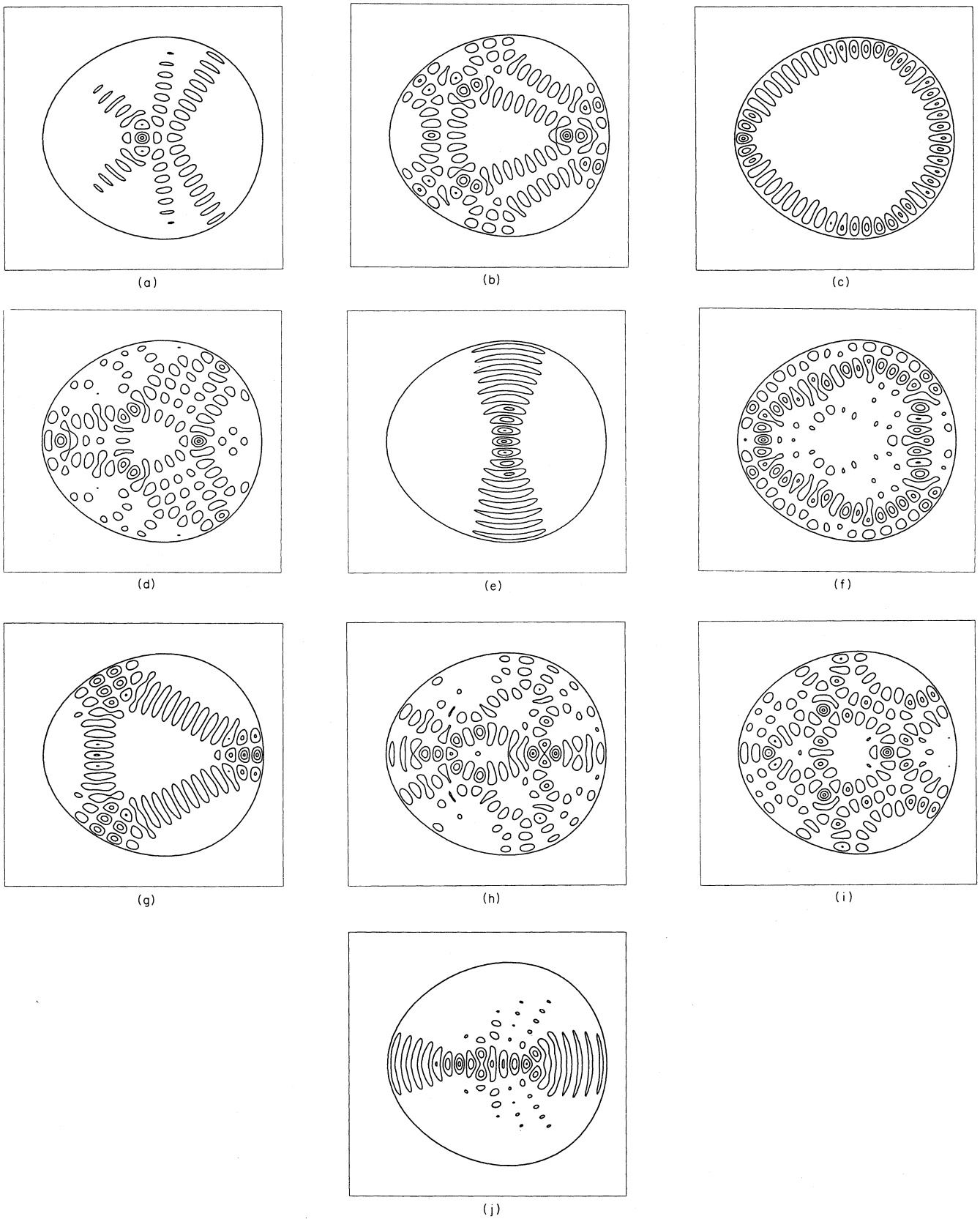

FIG. 2. Probability densities for 10 eigenfunctions of the deformed circular billiard $x^2+y^2+\epsilon x^3=1$, $\epsilon=0.2$. These are all the even eigenstates whose eigenvalues are in the range $30.0 \leq \sqrt{A}k \leq 31.3$. These states are ordered with increasing energy.

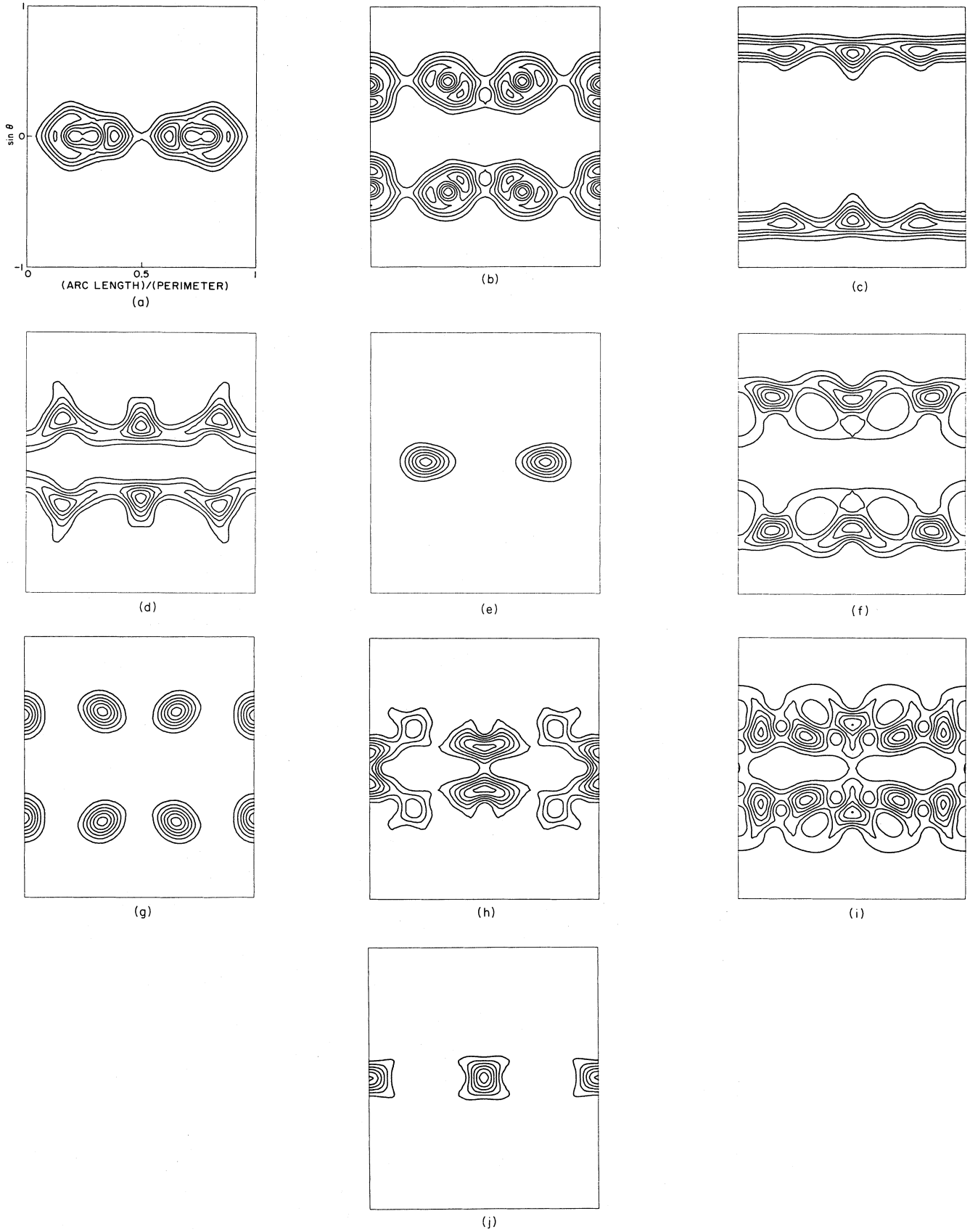

FIG. 3. Quantum Poincaré sections for the eigenstates shown in Fig. 2.

fined in phase space than in configuration space. Finally, the QPS's shown in Figs. 3(f), 3(h), and 3(i) spread over most of the chaotic basin, with some peaks that suggest the presence of an unstable 3-cycle in Fig. 3(f) and an unstable 5- cycle in Fig. 3(i). These periodicities are not apparent in Figs. 2(f) and 2(i).

V. DISCUSSION AND CONCLUSIONS

Quantum Poincaré sections have been previously introduced in periodically driven one-dimensional systems using the eigenfunctions of their associated evolution operator [13]. A Husimi representation of these eigenfunctions gives immediately an appropriate QPS for the problem. In billiards this is not possible, since there is no well-defined evolution operator to carry the dynamics on the one-dimensional s variable. In this case the simplest approach to the QPS is through the full configuration space eigenstates. For more general cases a procedure to obtain QPS's has been proposed [15], but our approach has the advantage of starting directly with the relevant 1D variable.

In the full 4D phase space of the billiard the Wigner functions for regular eigenstates are expected to be largest on the 2D classical stable tori (their projections are the caustics), and to oscillate strongly on the rest of the 3D energy-allowed manifold [17]. Here these oscillations are suppressed by the coarse graining provided by the Husimi distribution. Irregular eigenstates spread over the 3D energy surface with enhancements on some unstable periodic points, and avoid carefully the regions layered with stable tori. This behavior is quite difficult to visualize in the full 4D phase space, but can be seen clearly in the QPS provided here. The scarring is better defined in the QPS and allows us to distinguish periodic components in the wave functions that are not easily recognizable in configuration space.

ACKNOWLEDGMENTS

This work was started at the Institute for Nonlinear Sciences, University of California at San Diego. We wish to thank their members for their hospitality. We thank the University of Illinois Research Board and the National Center for Supercomputer Applications for providing us with computer time. This work was supported in part by the National Science Foundation under Grant No. PHY-87-01775.

* Present address: Istituto per la Ricerca Scientifica e Tecnologica, 38050 Povo (Trento) Italy.

† Present address: International Centre for Theoretical Physics, P.O. Box 586, 34100 Trieste, Italy.

[1] For a pedagogical review see M. V. Berry, Eur. J. Phys. **2**, 91 (1981).

[2] L. A. Bunimovich, Funct. Anal. Appl. **19**, 254 (1974).

[3] Ya. G. Sinai, Russ. Math. Surv. **25**, 137 (1970).

[4] V. F. Lazutkin, Math. USSR Izv. **7**, 185 (1973); R. Douady, thesis 3rd cycle, Université Paris VII, 1982.

[5] G. Benettin and J.-M. Strelcyn, Phys. Rev. A **17**, 773 (1978); M. Henon and J. Wisdom, Physica D **8**, 157 (1983).

[6] S. W. McDonald and A. N. Kaufman, Phys. Rev. Lett. **42**, 1189 (1979); Phys. Rev. A **37**, 3067 (1988).

[7] E. J. Heller, Phys. Rev. Lett. **53**, 1515 (1984), E. J. Heller *et al.*, Phys. Scr. **40**, 354 (1989).

[8] M. V. Berry, Ann. Phys. (N.Y.) **131** 163 (1981).

[9] M. Robnik, J. Phys. A **17**, 1049 (1984).

[10] G. D. Birkhoff, *Dynamical Systems* (American Mathematical Society, Providence, RI, 1927; reprinted 1966), Vol. IX.

[11] K. Husimi, Proc. Phys. Math. Soc. Jpn. **22** 246 (1940).

[12] M. Hillery *et al.*, Phys. Rep. **106**, 121 (1984).

[13] S.-J. Chang and K.-J. Shi, Phys. Rev. A **34**, 7 (1986).

[14] A. Perelomov, *Generalized Coherent States and Their Applications* (Springer-Verlag, New York, 1986).

[15] P. Leboeuf and M. Saraceno, J. Phys. A **23**, 1745 (1990).

[16] G. N. Watson, *A Treatise on the Theory of Bessel Functions*, 2nd ed. (Cambridge University Press, Cambridge, 1962).

[17] A. M. Ozorio de Almeida and J. H. Hannay, Ann. Phys. (N.Y.) **138**, 115 (1982).